PRINT ISSN 1119-8362
Electronic ISSN 1119-8362

Full-text Available Online at
https://www.ajol.info/index.php/jasem
http://ww.bioline.org.br/ja

J. Appl. Sci. Environ. Manage.
Vol. 24 (2) 197-206 February 2020

Assessment of Wound Healing Activity of Green Synthesized Titanium Oxide Nanoparticles using *Strychnos spinosa and Blighia sapida*

*[1]HASSAN, H; [1]OMONIYI, KI; [1]OKIBE, FG; [1]NUHU, AA; [2]ECHIOBA, EG; [3]EGWIM, EC

[1]*Department of Chemistry, Ahmadu Bello University, Zaria-Nigeria*
[2]*Department of Veterinary Medicine, Ahmadu Bello University, Zaria-Nigeria*
[3]*Center for Genetic Engineering and Biotechnology, PMB 65, Minna Niger State Nigerian*
**Corresponding Author Email: hussainahassan92@gmail.com*

ABSTRACT: The biosynthesis of nanoparticles has been proposed as a cost effective and environmentally friendly alternative to chemical and physical methods. The present work investigates the synthesis of titanium oxide nanoparticles (TiO_2 NPs) by green approach using *Strychnos spinosa* and *Blighia sapida* leave extracts. The detailed characterization of theTiO_2 NPs was carried out using UV-Visible Spectroscopy, Scanning Electron Microscopy (SEM), X- ray Diffraction (XRD), and Fourier-Transform Infrared (FTIR) Spectroscopy. The green synthesized TiO_2 NPs excitation was confirmed using UV–Vis spectrophotometer at 270 and 290 nm for *Strychnos spinosa and Blighia sapida* respectively. SEM revealed that the synthesized TiO_2NPs were spherical and crystalline in nature. The overall sizes are 40 and 50 nm for *Strychnos spinosa* and *Blighia sapida* respectively. FTIR spectroscopic analysisshowed the presence of flavonoids, polyphenols and amide groups likely to be responsible for the green synthesis of titanium oxide nanoparticles using*S. Spinosa* and *B .sapida* aqueous leaf extracts. The XRD pattern showed the characteristic Bragg peaks of (111), (200), (220) and (311) facets of the anatase titanium oxide nanoparticles and confirmed that these nanoparticles were crystalline and spherical in nature. Furthermore, the green synthesized TiO_2 NPs wound healing activity was examined in the excision wound model by measuring wound closure, histopathology and protein profiling. This revealed significant wound healing activity in Albino rats. In the present study, topical application ofnanoformulated extracts of *B. sapida*a nd *S. spinosa* significantly accelerated wound healing with 20% nanoformulated ointment having the highest percentage wound contraction ability comparable with gentamicin (a commercially sold antimicrobial agent used in dressing wounds). In conclusion, this work proved the capability of using TiO_2 NPs to deliver a novel therapeutic route for wound treatment in clinical practice.

DOI: https://dx.doi.org/10.4314/jasem.v24i2.2

Dates: Received: 16 November 2019; Revised: 11 January 2020; Accepted: 22 February 2020

Keywords: Wound healing activity; SEM; TiO_2; XRD; FTIR; UV–Vis spectroscopy.

One of the main objectives in wound healing is restoration in the shortest time with minimal side effects. Today, infection is considered as one of the main causes of mortality owing to wounds, especially after surgery. The management of these wounds is an ongoing problem which places a considerable drain on healthcare systems. Many microbiological studies have reported that *S.aureus*, streptococci and *P. aeruginosa* are the most frequently identified aerobic pathogens causing invasive wound infection. (Cho *et al*., 2005; Naheed *et al*., 2009; Shiriashi and Hirai 2008). *S. aureus* is a key human wound-infecting pathogen that interferes with cell functions of the host and causes delayed epithelial closure of the wound, possibly due to its interaction with fibronectin and inhibition of keratinocyte migration (Shah *et al.,* 2008). Antibiotic resistant bacterial strains with different mechanisms are found continually and thus new drugs are required (Bali *et al.,* 2006). Therefore, the finding of new antimicrobial agents with novel mechanisms of action is essential and extensively pursued in antibacterial drug discovery (Coates *et al.* 2002). Nanotechnology puts together the capabilities to manage the properties of materials by controlling their size range usually from 1-100nm (Prakash *et al.,* 2013). This has motivated carrying out research into numerous potential uses for nanomaterials. An ideal material should be able to protect wounds against microbial interactions. For centuries, metals and metallic oxides including silver, titanium and zinc have been applied as bactericidal and bacteriostatic agents, each with different properties and spectrums of activity. TiO_2 nanoparticles have become a new generation of advanced materials due to their novel and interesting optical, dielectric, and photo-catalytic properties from size quantization (Luo*et al.,* 2007).The present study was designed to determine the efficiency of TiO_2 NPs against microbial activityon surgically

**Corresponding Author Email: hussainahassan92@gmail.com*

induced full thickness skin wounds inoculated with *S. aureus* and deep bacterial load of wounds local infection in albino rat.

MATERIALS AND METHODS

Sample Collections: Fresh leaves of *B. sapida and S. spinosa* plants were collected from the biological garden of Federal Polytechnic, Bida (Latitude 9°4'60'' N, Longitude 6°1'0'' E), Niger State, Nigeria in 2017.

Preparation of the plant extract: The leaves of *B. sapida and S. spinosa* collected were thoroughly washed and rinsed in distilled water, and then room dried for two weeks. After which hands were used to break them into fine pieces. Then 500 g of each plant was smashed into 1000 ml of sterile distilled water in a gas jar and boiled at 60°C for 15mins and then filtered through Whatman No.1 filter paper. The percentage yield of the plant extracts are 16% and 15.5% for *B. sapida and S. spinosa* respectively. The aqueous extracts were stored at 40°C in an incubator for further experiments (Liu *et al*., 2013).

Phytochemical screening of plant extracts: The extracts were subjected to tests for secondary metabolites such as tannins, flavonoids, steroids, glycosides, alkaloids, glycosides and saponins. The tests were carried out using standard methods of analysis (Trease and Evans, 2002).Analyses were done in triplicate.

Synthesis of TiO_2 nanoparticles from the extracts: To prepare an aqueous solution of 1.0M $TiCl_4$, 5.0 ml of $TiCl_4$ was measured using a suction pipette, and mixed with 100 ml of distilled water in a 250 ml Erlenmeyer flask. The content was swirled properly. The mixture was then stored at 40°C before use. To a 100 ml portion of each of the leaf extracts of *B. sapida and S. spinosa,* 10 ml of the 1.0 M $TiCl_4$ solution was added in dropson a water bath at a constant temperature of 70°C for a period of 4 hours with constant stirring at 1000 rpm. The suspension produced was centrifuged at 2000 rpm for 20 mins and the supernatant liquid decanted.The residue was repeatedly washed with de-ionized water. Centrifugation, decantation and washing processes were repeated thrice to remove any impurity from the surface of the titanium oxide nanoparticles (Prakash*et al.,* 2013). The precipitate obtained was dried in an oven at a temperature of 40°C for 30 mins (Kalyani *et al.,* 2006). The synthesized titanium dioxide nanoparticle samples were then subjected to characterization by UV- Vis, FTIR, XRD and SEM.

Uv-vis spectrophotometry determination: About 10 ml each ofplant extracts, plant extracts mediated titanium oxide nanoparticlesand commercial TiO_2 nanoparticles sample in colloidal solutions were separately placed in the cell holder of a UV- Vis spectrophotometer (model UV 1800 Shimadzu, Japan), in order to determine the absorption spectrum of the sample using the range between 200 to 800 nm. Colloidal solution was obtained by mixing warm distilled water with synthesized TiO_2 (Liu *et al.,* 2013).

Fourier-transform infrared (FTIR) spectroscopy analysis: The determination of the functional groups on the surface of the plant extract mediated titanium oxide nanoparticles was investigated by using a FTIR spectrophotometer ((Perkin Elmer Spectrum 2, Germany), and the spectra were scanned in the range of 4000 – 400 cm^{-1} at a resolution of 4 cm^{-1}. The samples were prepared by dispersing each of the biosynthesized titanium oxide NPs and commercial TiO_2 nanoparticles uniformly in a matrix of dry KBr, and then compressed to form an almost transparent disc. KBr was used as a standard analyte for the samples (Dhadapani *et al.,* 2012).

Scanning electron microscopy (SEM) of the nanoparticle: In order to determine the surface morphology of the synthesized nanoparticle, SEM machine (HITACHI Model S-3000H Japan) was used. Thin films of the samples (biosynthesized titanium oxide NPs and commercial TiO_2 nanoparticles) were prepared on a carbon coated copper grid by just dropping a very small amount of each sample on the grid,; the film on the SEM grid was allowed to dry and the images of nanoparticles taken (Sundrarajan *et al.,*2011).

X ray diffraction (XRD) analysis of the nanoparticles: X-raydiffraction measurements of the biosynthesized titanium oxide NPs and commercial TiO_2 nanoparticles were recorded on X - ray diffractometer (Philips Analytical). The phase variety, particle size and material identification of the NPs were identified.The samples were taken in lids and put under instrument for analysis (Dhadapani *et al.,* 2012).

*In vivo (clinical) antimicrobial tests (Wound healing studies): Experimental animals***:** Healthy Albino rodents were purchased from Animal Breeding Unit of Biochemistry Department, Federal University of Technology, Minna, Niger State, Nigeria. The animals were kept in clean plastic cages and maintained under standard laboratory conditions. They were allowed unrestricted access to rat pellets and water. The study was carried out according to the Guide for the Care and the Use of Laboratory Animals of the Institute of Laboratory Animal Resources, Commission of Life Sciences, National Research Council, USA (ILAS, 1997).

Creation and contamination of excision wound: The dorsum of rats was shaved and disinfected with methylated spirit. Then, full thickness excision wounds were created following the method described by Morton and Malone (1992).For post wounding, the rats were randomly assigned into 6 groups of 5 animals per group. Then, using sterile Pasteur pipettes, wound on each animal was contaminated by flooding with 1 ml of standardized broth culture of *Staphylococcus aureus*. The animals were carefully placed in disinfected cages kept in a disinfected, clean and dust-free animal house in the Department of Biochemistry, Federal University of Technology Minna, Niger state, Nigeria. The wounds were not treated for 24 hr post contamination to ensure colonization and establishment of infection. Treatment of animal wound commenced 48 hr post contamination. Four treatment groups consisting of 5 animals per group were treated as follows: groups I and II were treated topically with 10% and 20% *B sapida and S. spinosa* leave extracts ointment respectively, groups III and IV were treated topically with 10% and 20% nanoformulated *B sapida* leaf extract mediated TiO_2 nanoparticle ointment respectively, groups V and VI were treatedtopically with 10% and 20% commercial TiO_2 nanoparticle ointment while groups V11 and VI11 were treated with gentamicin sulphate and sterile soft white paraffin, respectively. Treatment of the animals continued until complete healing occurred.

Percentage Wound Contraction: The wound diameter of each animal was measured at 3, 7, 10 and 14 days post wounding (dpw) using a transparent meter rule, and the percentage wound contraction calculated using the method of Ezike *et al*. (2010).

Determination of wound microbial load: At 3 and 14 days post-treatment (dpt), wound swabs from each animal was taken in duplicate using sterile swab sticks. The total viable count of the wound was determined following the standard plate counting method. Briefly, each swab was inoculated into sterile nutrient broth to make stock solutions which was used for double-fold (10^{-2}) dilutions. Using a sterile pipette, 0.1 ml of the 10^{-2} dilution was introduced on the surface of sterile nutrient agar and a sterile glass spreader was used for even distribution of the inoculum. The inoculated plates were incubated at 37°C for 24 hours and the colonies were counted (Ezikeet *al*. 2010).

RESULTS ANDDISCUSSION

Phytochemical Analysis: The preliminary phytochemical analysis was studied (Table1) and results showedthe presence of metabolites.Flavonoids and glycosides were present in both extracts of *S. spinosa* and *B. sapida*. While alkaloids and tannins were only present in *S. spinosa, saponins and steroids were only found in B. sapida*. This revealed pronounced importance of phytochemical compounds because the crude extracts possessed varied composition of secondary metabolites in the form of phytochemicals. Similar results were also reported by Salam *et al.* (2016) in the latex of *Calotropisprocera*. The pharmacological action of crude drugs and other therapeutic uses are due to their therapeutically active constituents such as tannins, flavonoids, alkaloids and several other aromatic compounds or secondary metabolites of plants which serve as defense mechanism against predation by many microorganisms, insects and herbivores. So, this phytochemical screening serves as initial step in predicting potential of active compounds.

Table 1 Qualitative phytochemical screening of the plant extracts.

Parameter	*S. spinosa*	*B. sapida*
Tannins	+ ve	- ve
Saponins	- ve	+ ve
Steroids	- ve	+ ve
Alkaloids	+ ve	- ve
Flavonoids	+ ve	+ ve
Glycosides	+ ve	+ ve

Physical Properties of Biosynthesized Blighasapida and Strychnosspinosa Mediated Titanium Dioxide: The biosynthesized *B. sapida and S. spinosa*mediated titanium dioxide nanoparticles were primarily confirmed by the contrast of colour changes of greenish to dark brown and reddish black colour for *B. sapida and Strychnosspinosa* mediated titanium dioxide nanoparticles respectively, indicating the synthesis of TiO_2 NPs. The generation of colour is due to excitation of surface plasmon in the metal nanoparticles. Similar results were also reported earlier for synthesis of titanium dioxide nanoparticles using *Azadirachtaindica* leaf extracts (Sankar *et al.,* 2015) and also with *C. sinensis* extract (Bali *et al.,* 2006). TiO_2 NPs were observed to be stable in solution (Ahmad *et al.,* 2016).

UV-Visible analysis: The UV–Vis spectroscopy was used to determine the formation and the stability of the synthesized titanium oxide nanoparticles in aqueous colloidal solution. It is also used to predict the initial phytoconstituents in plant material. The UV spectrum of the prepared biosynthsised TiO_2 nanoparticles and commercial titanium oxide Npsarepresented in Figure 1, 2 and 3 indicatingthat they all display maximum absorption in the vicinities of 400-800nm. The spectrum showed the formation of peak in the wavelength of 229 nm for the *B. sapida*mediated NPs, a peak in the wavelength of 231 nm for the *S. spinosa*-mediated counterpart, and a peak of 430 nm for commercial titanium oxide nanoparticles. The UV-Vis

spectra of plant extracts of biosynthsised TiO_2 nanoparticlesusing S. *spinosa* and *B. sapida* had high absorbance of 3.475 and 3.678 respectively compared tocommercial titanium oxide nanoparticles which had1.27. This was because the various metabolites from plant extract introduced to solution made the plasmon band broad and they may be read in the spectrophotometric range with surface plasmon resonance (SPR) which is responsible for exhibiting the absorption of UV-Vis radiation (Kim *et al*., 2013). These wave lengths arise due to the surface Plasmon resonance of the particle (Joshin *et al.,* 2008). The magnitude of peak, wavelength and spectral bandwidth associated with nanoparticles are dependent on size, shape and material composition (Prakash *et al.,* 2013, Kim *et al*., 2013). These changes in their properties increased their interacting faces thereby considered as enhancement in terms of absorbance spectrum in the UV-Vis region. Commercial TiO_2Nps had the least absorption as indicated in Figure 3.This was similar to the trend obtained by Salam *et al.*(2016) in the work done on synthesised *Citrus paradisi* peel extract mediated titanium dioxide nanoparticles andbiological synthesis of TiO_2 nanoparticles using extracts of *Ananascomosus* (Anwar *et al*., 2010;Wilkinson *et al*., 2011).

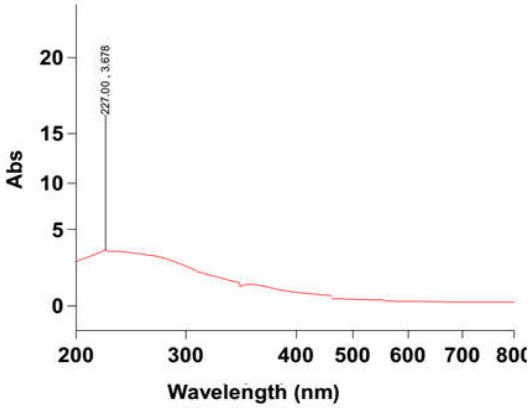

Fig 1: *UV-Vis spectrum of titanium oxide nanoparticles synthesized by Blighiasapida*

FTIR Analysis: FTIR analysis was used to find out the reduction of TiO_2 nanoparticles by phytochemical compounds present in the plant extracts. These compoundsare responsible for the reduction and stabilization of TiO_2 nanoparticles. Figure 4, 5 and 6 show the FTIR spectrum of *S. spinosa, B. sapidamediated* TiO_2 nanoparticlesand that of commercial TiO_2 NPs, respectively.

FTIR SpectralData Interpretation: B. sapida mediated TiO_2 NPs: B. ***sapida*** mediated TiO_2 NPs showed characteristic absorption bands at 3220cm $^{-1}$(hydroxyl (-OH) group), 1617cm $^{-1}$(for (C=O stretching), absorption at 1282 cm $^{-1}$(for C-N stretching) and at 1438 cm $^{-1}$for alkyl group.

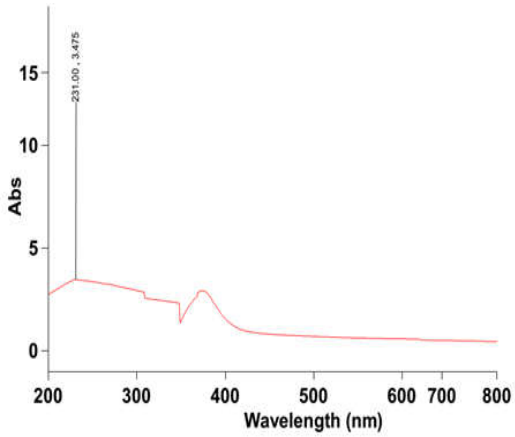

Fig 2: *UV-Vis spectrum of titanium oxide nanoparticles synthesized by S. spinosa*.

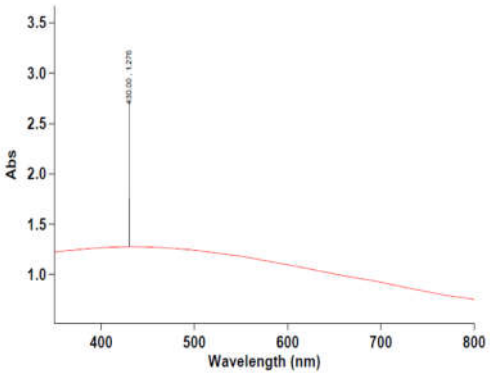

Figure 3: *UV-Vis spectra ofcommercial titanium oxide nanoparticles*.

S. spinosamediated TiO_2 NPs: The characteristic absorption bands were exhibited at 2920cm $^{-1}$(for C-H stretching) and at 1602.8 cm $^{-1}$for carbonyl group (C=O), and at 3678.9 cm $^{-1}$for Hydroxyl (-OH) group; Amineat 2920cm $^{-1}$and 1513 cm $^{-1}$for (C=C) stretching vibration.

Commercial TiO_2 NPs: Figure 6 indicated that characteristic absorption bands were exhibited at 3712–3768cm $^{-1}$ for hydroxyl (-OH) group and at 1654 cm $^{-1}$for carbonyl group (C=O) (Anwar *et al*., 2016). From the FTIR results, there were presence of hydroxyl groups of phenols, carbonyl group (C=O), alkyl group. Bali *et al.*(2006) reported same with amide group; these formedlayers on the nanoparticles and acted as capping agent andprovidedstability on extract of *N. tobacuum*leaves mediated silver NPs. The

functional groups in the FTIR results support the presence of phenolic compounds (flavonoids) in the extracts as evidenced by phytochemical analysis. Raymond *et al.* (2009) reported that the band at 1742 cm^{-1} is characteristic of stretching vibrations of the carbonyl functional group in ketones, aldehydes and carboxylic acids in the study on *Micrococcamercurialis*. Based on these FTIR studies, it can be suggested that the biomolecules present in the plant extract mediated TiO_2 Nps play dual role in formation and stabilization to TiO_2 nanoparticles.

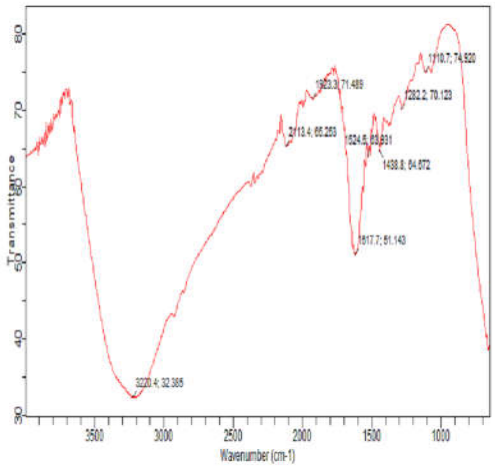

Fig 4: FTIR spectrum of titanium oxide nanoparticles prepared with B. sapida

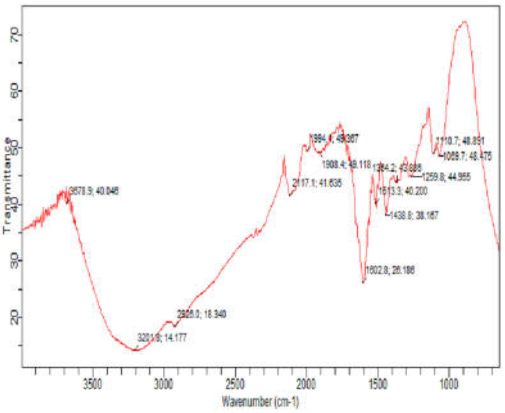

Fig 5: FTIR spectrum of titanium oxide nanoparticles prepared with S.spinosa.

Scanning Electron Microscopic analysis: Figure7, 8 and 9 show the SEM images of biosynthesised TiO_2 nanoparticles obtained using leave extracts of *S.* spinosa*, B. sapida* and commercial TiO_2 nanoparticles respectively. The images describe the surface morphology of the TiO_2 nanoparticles.

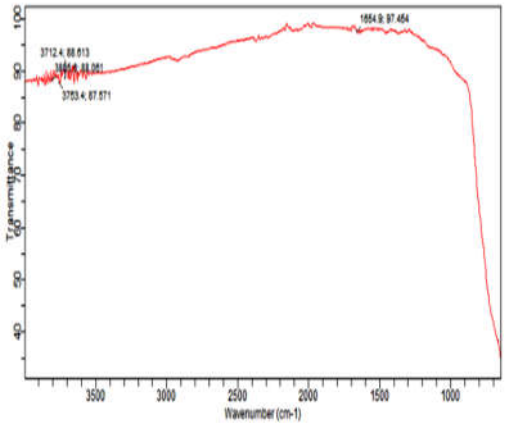

Fig 6: FTIR spectrum of commercial titanium oxide nanoparticles.

The green synthesized TiO_2 nanoparticles showed monodispersity without aggregation when compared to that of the commercial TiO_2 nanoparticles. This is due to the capping of TiO_2 nanoparticles with the compounds present in the leave extracts. The particles were found to be spherical with undifferentiated shapes.Previous reports showed that phytochemical compound in nanoparticles are disaggregated and are stable (Nour *et al.*, 2010). Prathna *et al*. (2010) supports the present findings in the work on *Origanumvulgare* aqueous leaf extract. It could therefore be speculated that the phytochemicals in these leave extracts coat the surface of the TiO_2 nanoparticles thus preventing their aggregation. The SEM images showed average sizes of 50 nm, 40 nm and 72nm for biosynthesized TiO_2 nanoparticles obtained using leave extracts of *S.* spinosa*, B. sapida* and commercial TiO_2 nanoparticles respectively. Titanium dioxide nanoparticles of approximate diameter of 50 and 60 nm have been previously reported (Raymond *et al.,* 2009). The TiO_2-NPs of these sizes showed that nanoparticles produced by this method were primarily crystallline (Singhal *et al.,* 2011; Ismagijov *et al.,* 2009). This is in agreement with previous reports fromAhmed *et al. (*2011).

X-ray Diffractometric analysis (XRD): The X-ray diffraction was used to confirm the chemical composition and crystalline nature of the synthesized nanoparticles. The XRD pattern of TiO_2 nanoparticles obtained using leave extracts of *B. sapida, S. spinosa,* and commercial TiO_2nanoparticles are shown in Figure 10, 11 and 12 respectively. A sharp diffraction peak was observed in Commercial TiO_2 nanoparticles, whereas, the intensity of diffraction peak of green synthesized TiO_2 nanoparticles are less with slight broadening. The intense sharp peak indicated that the

crystalline phase of anatase TiO_2 was successfully formed (Ismagijov *et al.,* 2009).

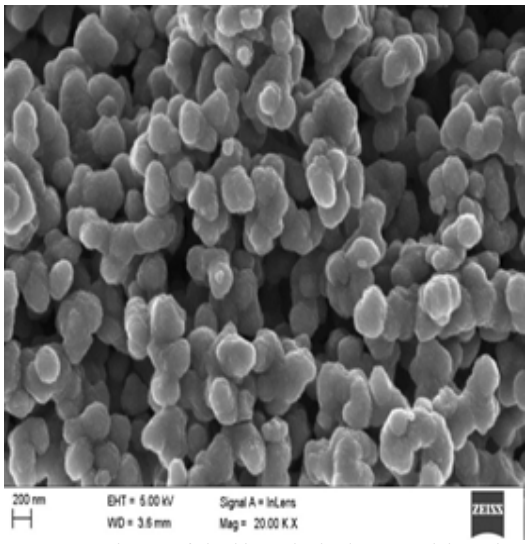

Fig 7: SEM image of the biosynthesized nanoparticles using *B. sapida extracts*

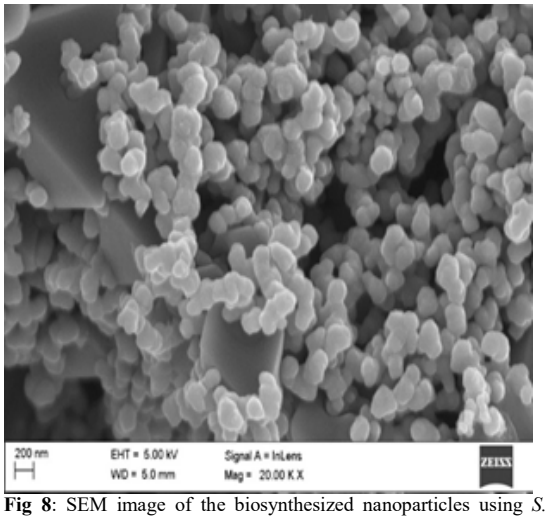

Fig 8: SEM image of the biosynthesized nanoparticles using *S. spinosa extract.*

X-ray Diffractometric analysis (XRD): The X-ray diffraction was used to confirm the chemical composition and crystalline nature of the synthesized nanoparticles. The XRD pattern of TiO_2 nanoparticles obtained using leave extracts of *B. sapida, S. spinosa,* and commercial TiO_2nanoparticles are shown in Figure 10, 11 and 12 respectively. A sharp diffraction peak was observed in Commercial TiO_2 nanoparticles, whereas, the intensity of diffraction peak of green synthesized TiO_2 nanoparticles are less with slight broadening. The intense sharp peak indicated that the crystalline phase of anatase TiO_2 was successfully formed (Ismagijov *et al.,* 2009).

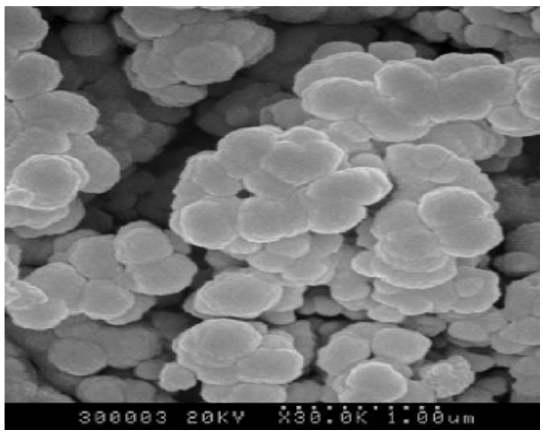

Fig 9: SEM image of the Commercial TiO_2 Nps.

The XRD pattern exhibited eight prominent peaks with 2Θ at around 25.32°, 37.72°, 48.10°, 53.82°, 55.09°, 62.71°, 75.03° and 82.83°, indexed to the TiO_2anatase values (101), (004), (200), (105), (211), (204), (215) and (224), respectively. The crystallite size for the prepared samples was determined by measuring the broadening of a most intense peak of the phase (main peak) in a diffraction pattern according to Debye-Scherrer equation as follows:

$$D = \frac{K\lambda}{\beta\cos\theta}$$

Where D is the crystallite size of the particle, θ is the Bragg diffraction angle, β is the full width at half-maximum (FWHM), λ is the wavelength (0.15418 nm) and k (0.94) is a constant. Theintensity of the diffraction peak of the green synthesised TiO_2 nanoparticles was broadened, whereas the peak of commercial TiO_2 nanoparticles was comparatively sharp. Ahmed *et al.* (2016) have reported the correlation between XRD peak broadening and the size reduction during green synthesis protocol. Thus, the broadening of XRD peak of biosynthesized TiO_2 nanoparticles observed in the study confirmed the size reduction. The XRD peak of commercial TiO_2 nanoparticles is sharp, thus indicating that their size is still larger than the green synthesised TiO_2nanoparticles.

Phytochemicals present in the leave extract of*S. spinosa, and B. sapida* would have coated the surface of the TiO_2 nanoparticles, resulting in decreased intensity in XRD peak. This phytochemical coating may enhance the stability of the nanoparticles, which in turn may enhance their bioavailability, making them suitable for biological applications. Commercial TiO_2 nanoparticles on the other hand showed comparatively

high intense peaks, clearly indicating that they are uncapped. These results are in agreement with the report of Ahmed *et al.* (2016) and Singhal *et al.*(2011).The XRD patterns obtained were matched with the database of JCPDS No: 21-1272; the crystallite size obtained by using this formula ranged between 40 nm and 50 nm for the synthesised TiO_2 nanoparticles. The result of this study is similar to that obtained for the synthesis of titanium dioxide nanoparticles mediated with aqueous leaf extract of *Ecliptaprostrata* that recorded crystallite size in the range of 36 to 68 nm with an average grain size of 49.5nm (Kim *et al*., 2013).

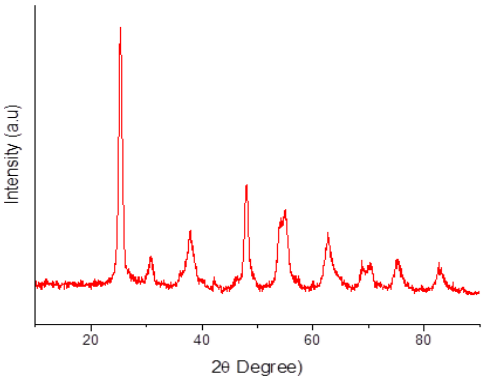

Fig 10: XRD images of biosynthesized TiO_2 NPS using*B. Sapida*extract.

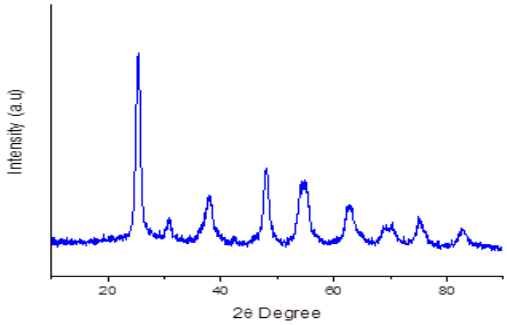

Figure 11: XRD images of biosynthesized TiO_2 NPS using*Sspinosa* extract.

Wound healing activity: Wound healing according to Al-Henhena *et al*. (2011) is a complex and dynamic process by which cellular structures and tissue layers in a damaged tissue restores itself as closely as possible to its original state. Results of the control and green synthesized TiO_2 NPs treated wounds on different days are presented in Table 2. The wound treated with synthesized TiO_2NPs indicated no evidence of pus formation, bleeding and microbial infections at any times and wounds heal without any complications whereas the control rats showed persistent inflammation

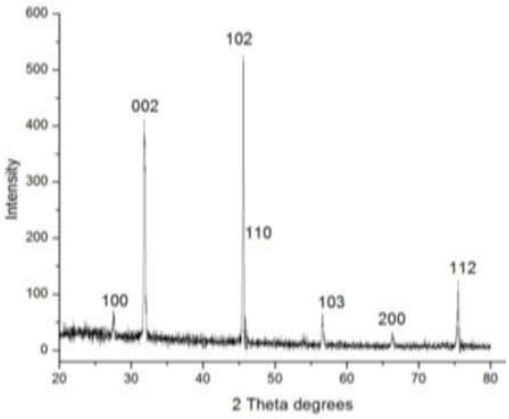

Fig 12: XRD of commercial TiO_2 nanoparticles.

The TiO_2 NPs treated wound revealed a significant wound contraction on 4thday onwards and the upcoming days wound closure was much faster when compared with control animals. On the 14thday the TiO_2 NPs treated animals showed most wound closure (94 %), while control animals exhibited 86 % wound closure. Significant wound closure and reduced wound size in the treated animals demonstrates the efficacy of green synthesized TiO_2 NPs on wound healing agent (Bidgoli *et al*., 2013; Matei *et al*., 2008). Topically administered TiO_2 NPs are effective in faster wound closure which might be due to the large availability, enhanced fibroblasts and collagen action in regenerated wound tissues (Tian *et al.*, 2007; Bidgoli *et al*., 2013). Myofibroblasts are believed to play a key role in wound contraction by exerting tension on surrounding extracellular matrix and secreting collagen which stabilizes the contraction (Sun *et al*., 2014).

Furthermore, the high surface area to volume ratio endows nanostructures with unique features contributed to the healing activities.For example, nanoscale particles provide a high probability of interaction with the biological target and an enhanced penetration into the wound site. As a result, nanoparticles have an ability to deliver a sustained and controlled release of therapeutics that result in an accelerated healing process. In view of the above reports, the wound contraction and healing effects of TiO_2 NPsusing *S. spinosa and B. sapida* might be attributed to phytochemical substances present which are known to promote wound healing. The understanding and control of microbial infection of wounds is very important for better healing and its management (Campostrini *et al.,* 2003*)*. Post-operative wounds are usually infected by bacterial organisms *(*Deshmukh *et al., 2009)*. The significant decreases in wound bacterial load in the treated groups

suggest that the extract and TiO_2 NPs synthesized has *in vivo* antibacterial effect against *Staphylococcus aureus* which is involved in wound contamination. The TiO_2 NPs synthesized by the extracts were able to reduce wound bacterial load comparable to the reference drug, gentamicin. Signs of bacterial infection of wounds include delay in the onset of the proliferative and re-modelling phases of wound healing process due to the release of free radical and lytic enzymes at the wound site *(*Eming *et al.,* 2007). The absence of irritation and/or pain at wound site during treatment and the significant increase in the rate of wound contraction and wound re-epithelialization is a reflection of good antibacterial potentials of the TiO_2 NPs as showed in the *in vivo* and *in vitro* antibacterial assay results. The antibacterial activity exhibited by theleave extracts could be attributed to the phytochemical constituents present in these extracts. (Eming *et al.,* 2007).

Table 2: Percentage wound contraction in rats post infliction of excision wounds

	Days			
	3	**7**	**10**	**14**
10% *S. spinosa*	5.54±0.87^{b}	34.98±2.34^{b}	67.45±3.45^{b}	75.43±4.45^{b}
20% *S. spinosa*	6.32±0.42^{b}	38.47±3.45^{b}	69.56±4.32^{b}	77.65±3.45^{b}
10% Nanoformulated- *S. spinosa*	4.56±0.32^{ab}	43.67±2.34^{bc}	76.67±3.45^{c}	89.56±2.09^{c}
20% Nanoformulated- *S. spinosa*	7.65±0.67^{c}	52.26±3.45^{c}	84.56±3.74^{c}	100.00±0.00^{d}
Gentamicin ointment	6.54±0.32^{b}	55.43±2.35^{c}	88.23±5.45^{c}	100.00±0.00^{a}
Negative control	2.67±0.12^{a}	22.34±1.45^{a}	41.56±1.45^{a}	66.78±4.56^{a}

Data are expressed as Mean ±SEM of five determinations. Values followed by different superscript alphabets were significantly different ($p<0.05$).

Conclusion: The TiO_2 nanoparticles synthesized from the *S. spinosa and B. sapida* leaf extracts were analysed for their antimicrobial activities. Synergistic antimicrobial activitiesof TiO_2 nanoparticles were proved in vivo through treatment of a case of wound caused by *Staphylococcus aureus* infection in Albino rats. The results of this study introduced remarkable in vivo TiO_2.NPs accelerating effects on the treatment of *S. aureus* infected skin wounds with no obvious side effects in the rats. To our knowledge, this therapy has not been investigated before. It has proved efficient and promising in managing infections caused by *S. aureu s*bacteria and it could be used as an alternative to conventional antibiotic therapy.

REFFERENCE

Ahmed, S; Ahmad, M; Swami, B.L and Ikram, S. (2016). A review on plants extract mediated synthesis of silver nanoparticles for antimicrobial applications: a green expertise. *Journal of Advance Res,* 7, 17–28.

Al-Henhena, N; Mahmoood, A.A; Al-Magrami, A; Nor, S.A.B; Zahra, A.A; Summaya, M.D; Suzi, M.S; Salmah, I: (2011). Histological study of wound healing potential by ethanol leaf extract of Strobilanthes crispus in rats. *J Med Plants Res*., 5 (16): 3666-3669.

Anwar, N.S; Kassim, A; Lim, H.N; Zakarya, S.A and Huang, N.M. (2010). Synthesis of Titanium Dioxide Nanoparticles via Sucrose Ester Micelle-Mediated Hydrothermal Processing Route. *Sains Malaysiana*, 39 (2): 261-265.

Bali, R.; Razak, N.; Lumb, A. and Harris, A.T. (2006).The synthesis of metallic nanoparticles inside live plants.*Laboratory for Sustainable Technology, School of Chemical and Biomolecular Engineering.*

Bidgoli, SA; Mahdavi, M; Rezayat, S.M; Korani, M; Amani, A; Ziarati, P. (2013) Toxicity assessment of nanosilver wound dressing in Wistar rat. *Acta Med Iran*. 7:203–8.

Campostrini, R; Ischia, M; Palmisano, L. (2003). Pyrolysis study of Sol-gel derived TiO_2 powders: Part I. TiO2- anatase prepared by reacting titanium (IV) isopropoxide with formic acid. *J. Therm. Anal. Calorim.* 71 (3): 997- 1010.

Cho, K; Park, J; Osaka, T; Park, S; 2005.The study of antimicrobial activity and preservative effects of nanosilver ingredient. *Electrochim. Acta*, 51: 956–960

Coates, A.; Hu, Y.; Bax, R.; Page, C. (2002). The future challenges facing the development of new antimicrobial drugs. *Nat. Rev. Drug Discov.1*, 895-910.

Eming, S; Martin, A.; Tomic-Canic MP. (2017). Wound repair and regeneration: mechanisms, signaling, and translation. *Sci. Transl .Med*. 6, 265sr266–265

Ezike, AC; Akah, P.A; Okoli, C.O; Udegbunam, S; Okuma, N; Okeke, C; Iloani O (2010) Medicinal plants used in wound care: a study of

Prosopisafricana (Fabaceae) stem bark. *Indian Pharm Sci*., 72 (3): 334-338.

Ismagilov, ZR; Tsykoza, L.T; Shikina, N.V; Zarytova, V.F; Zinoviev, V.V and Zagrebelnyi, S.N. (2009). Synthesis and stabilization of nano-sized titanium dioxide. *Russ. Chemistry Research*, 78 (9) 1-13. 43.

Kalyani, G; Anil, V.G; Bo-Jung, C; Yong-Chien, L. (2006) Preparation and characterization of ZnO nanoparticles coated paper and its antibacterial activity study. *J Green Chem.* 8: 1034 1041.

Kim, D.H; Ryu, H.W; Moon, J.H; and Kim, J. (2013). Effect of ultrasonic treatment and temperature on nanocrystalline TiO2 .*Journal of Power Sources*, 163 (1): 196-200.

Liu, C.M; Guo, L; Xu, H.B; Wu, Z.Y; Weber, J. (2013) Seed mediated growth and properties of copper nanoparticles, nanoparticle 1D arrays and nanorods. MicroelectronicEngineering. 66: 107-114.

Luo, P.G;Tzeng, T.R;, Shah R.R;Stutzenberger, F.J.(2007)Nanomaterials for Antimicrobial Applications and Pathogen Detection. *Curr Trends in Microbiol*; 3:111-128

Matei, A; Cernica, I; Cadar, O; Roman, C; Schiopu, V. (2008). Synthesis and characterization of ZnO – polymer nanocomposites. *Int J Mater Form*, 1: 767-770.

Morton, J.J; Malone, M.M: Evaluation of vulnerary activity by open wound procedure in rats. *J Trauma*. 1992, 20 (4): 323-324

Naheed, A; Singh, V.N; Salman, F.S. Seema, S. (2009). Ocimum Mediated Biosynthesis of Silver Nanoparticles. In: *ICMENS'09 Proceedings of the 2009 Fifth International Conference on MEMS NANO, and Smart Systems,* 80-84.

NCCLS, (2002). "Performance Standards for Antimicrobial SusceptibilityTesting," 12thInformational SupplementM100-S12, National Committee for Clinical Laboratory Standards, Villanova, PA.

Prakash, P; Gnanaprakasam, P; Emmanuel, R; Arokiyaraj, S; Saravanan, M. (2013). Green synthesis of silver nanoparticles from leaf extract of Mimusopselengi, Linn for enhanced antibacterial activity against multi drug resistant clinical isolates. *Colloids Surf*. B.; 1:255–9.

Prathnaa. V; Chandrasekarana, N; Raichurb, A.M. (2010). *Colloids and Surfaces B: Biointerfaces.* (82) 152–159.

Raymond, F.H.J; Nianqiang, W; Dale, P; Mary, B; Michael, W; Andrij, H. (2009).Particle length-dependent titanium dioxide nanomaterial toxicity and bioactivity. Part. *Fibre Toxicol.* 6 (12): 1-11.

Salam, H.A.; Rajiv, P.; Kamaraj, M Kudhier, M.A. (2016). Synthesis and photocatalytic activity of TiO_2 nanoparticles prepared by sol–gel method. *Journal of Solution Gel Sci. Technol.* 78:299-306.

Sankar, R.; Rizwana, K.; Shivashangari, K.S. and Ravikumar, V. (2015). Ultrarapidphotocatalytic activity of *Azadirachtaindica* engineered colloidal titanium dioxide nanoparticles. *Applied. Nanoscience*, 5:731- 736.

Sawai, J. (2003). Quantitative evaluation of antibacterial activities of metallic oxide powders (ZnO, MgO and CaO) by conductimetric assay. *J Microbiol Methods,* 54:177-182

Shah, M.S.A; Nag, M; Kalagara, T; Singh, S; Manorama, S.V. (2008). Silver on PEG-PU-TiO_2 polymer nanocomposite films; an excellent system for antibacterial applications. *Chem. Mater*, 20(7):2455-2460.

Shiraishi, Y; Hirai, T. (2008).Selective organic transformations on titanium oxide-based photocatalysts. *Journal of Photochemistry and Photobiology C: Photochemistry Reviews,* 9:157–170.

Singhal, G; Riju, B; Ashish, R.S. Rajendra, P.S. (2011). Eco-friendly Biosynthesis of Gold Nanoparticles Using Medicinally Important *Ocimum basilicum* Leaf Extract. *Adv. Sci. Engg. Med*., 4: 62-66.

Sundrarajan, M. Gowri, S. (2011). Green synthesis of titanium dioxide nanoparticles by *Nyctanthes arbor-tristis* leaves extract. *Chalcogenide Lett*., 8 (8): 447-451.

Sun, B. K.; Siprashvili, Z.; Khavari, P. A. (2014).Advances in skin grafting and treatment of cutaneous wounds. Science, 346, 941–945

Tian, J; Wong, K.K; Ho, C.M; Lok, C.N; Yu, W.Y; Che, C.M; Chiu, J.F; Tam, P.K. (2007). Topical delivery of silver nanoparticles promotes wound healing. *Med. Chem*.; 2:129–36.

Trease, G.E; Evans, W.C. (2002). Phytochemical Screening and In vitro Bioactivity of Cnidoscolus, 15th ed., pp. 211242, *WB Saunders, Edinburgh*.

Wang, W; Lenggoro, I.L; Terashi, Y; Kim, T.O; Okuyama, K. (2005).One-step synthesis of titanium oxide nanoparticles by spray pyrolysis of organic precursors. *Material Science Engineering,* 123 (3): 194-202.

Wilkinson, LJ; White, R.J; Chipman, J.K. (2011). Silver and nanoparticles of silver in wound dressings: a review of efficacy and safety. *J Wound Care*. 20:543–9.